Journal of Power Sources 196 (2011) 2013–2019

Contents lists available at ScienceDirect

Journal of Power Sources

journal homepage: www.elsevier.com/locate/jpowsour

Automatic control of load increases power and efficiency in a microbial fuel cell

Giuliano C. Premier[a,*], Jung Rae Kim[a], Iain Michie[a], Richard M. Dinsdale[b], Alan J. Guwy[b]

[a] Sustainable Environment Research Centre (SERC), Faculty of Advanced Technology, University of Glamorgan, Pontypridd, Mid-Glamorgan CF37 1DL, United Kingdom
[b] Sustainable Environment Research Centre (SERC), Faculty of Health, Sport and Science, University of Glamorgan, Pontypridd, Mid-Glamorgan CF37 1DL, United Kingdom

ARTICLE INFO

Article history:
Received 10 August 2010
Received in revised form
15 September 2010
Accepted 21 September 2010
Available online 1 October 2010

Keywords:
Microbial fuel cell
MFC
Control
Power
Coulombic efficiency
Optimisation

ABSTRACT

Increasing power production and coulombic efficiency (CE) of microbial fuel cells (MFCs) is a common research ambition as the viability of the technology depends to some extent on these measures of performance. As MFCs are typically time varying systems, comparative studies of controlled and un-controlled external load impedance are needed to show if control affects the biocatalyst development and hence MFC performance. The application of logic based control of external load resistance is shown to increase the power generated by the MFC, when compared to an equivalent system which has a static resistive load. The controlled MFC generated 1600 ± 400 C, compared to 300 ± 10 C with an otherwise replicate fixed load MFC system. The use of a parsimonious gradient based control was able to increase the CE to within the range of 15.1–22.7%, while the CE for a 200 Ω statically loaded MFC lay in the range 3.3–3.7%. The controlled MFC improves the electrogenic anodic biofilm selection for power production, indicating that greater power and substrate conversion can be achieved by controlling load impedance. Load control ensured sustainable current demand, applied microbial selection pressures and provided near-optimal impedance for power transference, compared to the un-controlled system.

© 2010 Elsevier B.V. All rights reserved.

1. Introduction

The performance of microbial fuel cells (MFCs) depends on coupled biological, chemical, electrical and physical processes, which together are time varying, nonlinear and spatially distributed. The arrangement of these processes in an MFC and their interaction determines the performance of the MFC. However, most of the research to improve the performance of MFCs has focused on reducing overpotential losses, through the selection of the electrogenic biofilm [1,2], substrate (fuel) [3], system design [4] and operating parameters without considering dynamics and the interactions between these factors [5].

Maximizing the power produced from an MFC by selecting the load has been considered previously [6]; however this has typically involved *pseudo*-static loads, using fixed resistances. A frequently used technique of determining the peak of the power curve (by, e.g. discharge curves or Tafel plot) [7], to establishing the current and hence load at which notional peak power is produced, will not in general allow persistent optimal power production. This is because MFC performance is time varying and often, the measurement procedure itself, will affect the biocatalyst [8], implying that current operating conditions affect future performance.

Altering electrical load in order to affect the power produced by an MFC has shown considerable promise and is almost ubiquitous in selecting static electrical loads for MFCs. Lyon et al. [9], were able to demonstrate that altering the external loading of MFCs would affect the anode biofilm community which develops, but the different communities exhibited similar performances in terms of power production. While this does not prove that manipulation of the load can deliver improved performances beyond those expected from static loads, it does indicate that a relationship exists between biofilm ecology and load resistance. Woodward et al. [10] employed a more sophisticated load varying technique using an optimisation algorithm based on a Multiunit Optimisation Method for maximum power point tracking (MPPT). In this work, rapid convergence on the maximum power was addressed using, two replicate MFCs to inform a MPPT algorithm [11,12]. However, the tracking rate for maximum power can only proceed at the rate which peak power varies, which in turn is dictated by the natural growth and establishment of the active electrogenic biofilm processes. Pinto et al. [13], presented a two population model which they were able to parameterise and validate with data from four MFCs. Their model indicated that small deviations between internal and external impedance in MFCs could cause large power losses and so concluded that in long term operation, external load should be 'at least periodically adjusted' in order to avoid methanogenic activity becoming problematic and therefore, ideally MPPT should be used.

The time varying nature of MFCs is evident particularly if considered from start-up with inoculation of the system. Consideration of an MFC model [14] confirms the nonlinearity and time varying dynamic behaviour of such systems [13]. By virtue of the biologically open characteristics of devices, for example applied to

* Corresponding author. Tel.: +44 1443 482333; fax: +44 1443 482169.
E-mail address: gcpremier@glam.ac.uk (G.C. Premier).

0378-7753/$ – see front matter © 2010 Elsevier B.V. All rights reserved.
doi:10.1016/j.jpowsour.2010.09.071

wastewater treatment or energy generation from non-sterile substrates, MFCs may also display a degree of stochastic behaviour as found in other open systems [15]. The potential of the anode will also affect start-up, as shown in [16,17], using artificially poised electrode potentials. This is typically done using an electrochemical interface, however alternatives which alter the external load applied to the MFC are possible, as demonstrated in this paper and by, e.g. [10,18]. It is then a relatively simple matter to vary this load in response to a control action.

Persistent optimal operation of the MFC at the maximum power point might be expected to deliver a stable and strengthening performance as the biofilm is continually selected for electrogenesis. Increasing power output may be expected to continue to the point where the system specific global maximum is reached, unless deleteriously perturbed. Depletion of the substrate, for example, would cause a diminution of maximum power from the MFC, as would substantive overloading of the MFC.

Therefore, controlling the load in real time is desirable in order to maintain sustainable electrical loading on the electrogenic biofilm. Otherwise, the biofilm which develops, may to a varying extents, loose activity in favour of non-electrogenic bioprocesses. Continual optimisation of the MFC may supply a selective pressure which will drive the electrogenic population to higher performance, as well as reducing side reactions such as methanogenesis and biomass production [19].

This paper addresses the control of power drawn from an MFC and the performance enhancement that results from dynamic control of load resistance. A parsimonious control strategy is investigated, which can advantageously be implemented using several low cost silicon based integrated circuit technologies. The control is able to optimise the power drawn from the MFC as the system varies with time, using simple Boolean logic to control the load impedance applied to an MFC. The power at any time is close to optimal, in the sense that peak power is drawn from the MFC and can be sustained at varying rates of current delivery without catastrophic system failure or avoidable loss of performance. The paper shows that the persistent selective pressure causes the instantaneous power optimum of the cell to alter with time, and so a near global optimum might be achieved. In so doing the control system is able to generate more power at a higher efficiency than a replicate, though un-controlled MFC that is subject to a static electrical load.

2. Materials and methods

2.1. MFC construction and operation

Duplicate H-type MFCs were constructed using two media bottles (320 ml capacity, Corning Inc., NY), joined by a glass tube containing a 2.1 cm diameter cation exchange membrane (CMI-7000, Membrane International Inc., USA) as previously described [20]. Anode and cathode electrodes were made of plain porous carbon paper (TGPH-120, Toray carbon paper, E-TEC, 2.5 cm × 4.5 cm, projected area of 22.5 cm^2). The ferricyanide solution (100 mM in phosphate buffer, 100 mM, pH 7) was used as catholyte in order to maintain cathode potential. The reactors were inoculated with a 10% digestion sludge (Cog Moors wastewater treatment plant, Wales, UK), and were operated in batch mode, being fed with 5000 mg l^{-1} acetate on a weekly basis before the start of the experiment. One of the duplicate MFCs was load controlled by connecting it to a monitoring and control system through an analogue/digital interface. Real-time dynamic monitoring and control were applied using an algorithm executed on a personal computer, as described below (load controlled MFC, LC-MFC). The second MFC reactor was connected to a static load (200 Ω) and monitored, but not controlled (static load MFC, SL-MFC). Both MFCs were operated in batch mode with magnetic stirring and at room temperature (ranging between 15 ± 2 °C and 30 ± 2 °C).

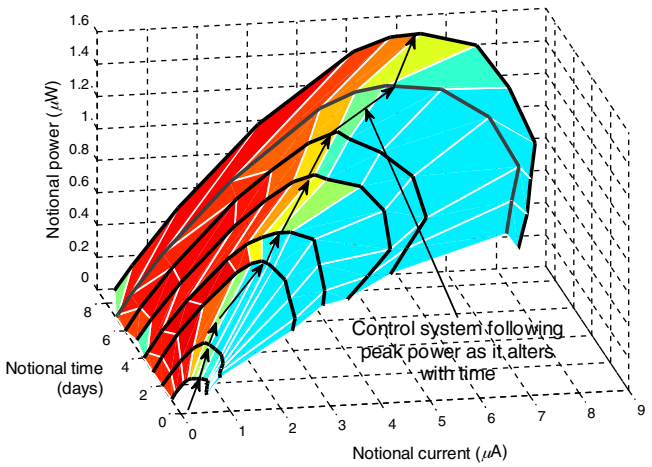

Fig. 1. Illustrative representation of controlled operating conditions optimising power generation as characteristic power distribution changes with time.

2.2. Control strategy

The control strategy implemented in this study is based on the hypothesis that an MFC will typically have a variable power curve with a single maximum at any time instant ($t > 0$), where t_o is the time at which the MFC is inoculated. The development of power curves can be plotted with axes of current (i), power (P), and time (t). A simple algorithm which is capable of tracking the peak power 'ridge' as it develops and alters over time as illustrated in Fig. 1. The peak power also varies with other operational parameters such as organic loading rate, pH, biofilm formation and temperature. The objective of the control strategy is to maintain a suitable operating current through dynamic control of an external load, which will therefore virtually optimise the instantaneous power generation with changing operating conditions.

The rate of change of power with current can be used to determine the required change of external load in order to 'search' for the peak power. The sign of the gradient of the power vs. current, $Si = sign(\partial P/\partial i)$ may be used to determine whether the load resistance should decrease or increase at each sample instant. The power generated by the MFC is assumed to be equal to the power dissipated in an external load, which may be determined by measuring the voltage (V) across the load, such that power $P = V^2/R$. Boolean logic is applied such that if the power is increasing, i.e. if $Pt = sign(\partial P/\partial t) > 0$ (logic 1) and the slope of the power curve $Si > 0$ (logic 1), then resistance R *is* reduced by a single step (10 Ω) of a digital potentiometer. Other scenarios are dealt with in a similar manner as presented in Table 1. The Boolean algebra resulting from

Table 1
Truth table for MFC peak power search logic control strategy.

Si	*Pt*	A Load resistance reduced	B Load resistance increased	C Load resistance unchanged
0	0	0	1	0
0	1	1	0	0
1	0	0	1	0
1	1	1	0	0
0	–	0	0	1
1	–	0	0	1

Table 1 may be written as in Eq. (1):

$$\begin{aligned} &A = (\overline{Si} \wedge Pt) \vee (Si \wedge Pt) \\ &B = (\overline{Si} \wedge \overline{Pt}) \vee (Si \wedge \overline{Pt}) \\ &else \\ &C = 1 \end{aligned} \quad (1)$$

It is necessary to determine *Si* and *Pt*, which is achieved in this study by using a first order backward finite difference approach, given that only a single data point needs to be stored. The load resistance is then increased, reduced or maintained constant, to an appropriately defined resolution for the subsequent sampling period.

The measured potential was used to calculate the power dissipated in the load, which was then digitally filtered. The maximum power transfer would occur when the internal and external load impedances of the MFC were matched, and at low frequencies such as those experienced, the internal resistance and load resistance would be expected to be virtually the same at steady state, i.e. after filter and system transients subside.

2.3. Implementation of control system

The control strategy was implemented by using a single CMOS Intersil® 100 step 1 kΩ digitally controlled potentiometer, X9C102 (Farnell UK Ltd., Leeds) as the load resistance. The potentiometer provides 100 wiper tap points giving 10 Ω resolution at each step change. This device is controlled via a 3 terminal serial interface and has a specified end-to-end tolerance of ±20% and typical wiper resistance of 40 Ω, which defines the minimum resistance. The X9C102 device was initialized by ensuring the resistance was at zero (by stepping resistance down 100 times), before incrementing to a desired starting resistance selected using *a priori* knowledge of the microbial fuel cell employed.

The Boolean logic control algorithm was implemented using a PC equipped with the programming language G, and an analogue and digital data acquisition card. Thus, the control strategy along with MFC voltage monitoring, signal processing and data storage were all implemented in a virtual instrument (VI) programmed in LabVIEW™ and interfaced to the MFC by a NI USB-6009 DAQ card (National Instruments, Newbury, UK). The system was sampled and control actuations were taken at 1 min intervals in accordance with the logic presented above. The partial derivatives *Si* and *Pt* were determined over 2 data samples.

2.4. Analysis of biofilm ecology

Anodic biofilms were examined at the end of the experiment to investigate and compare the influence of control on the MFC microbial ecology, which had developed over almost 600 h. LC-MFC and the SL-MFC reactors were operated anaerobically and identification of 16S rDNA and PCR analysis were performed as previously described [21] (see Supplementary Information for details of methods and primers used).

DNA was quantified with a NanoDrop(TM) spectrophotometer (Thermo Fisher Scientific Inc., USA) and the concentration and purity of the DNA (characterized by 260/280 nm absorbance ratio) was documented.

Scanned DGGE gels were analysed using GelCompar II software (Applied Maths, Belgium). Test bands were viewed and compared in terms of intensity and position. To correct for variations in successive DGGE gels a standard marker sample was run with each gel, this was used to normalise the bands based on defined reference positions. Densitometric curves were calculated for each gel track using a best-fitting Gaussian algorithm for each band.

Microbial ecological analysis of the DGGE band profiles archaeal and bacterial communities were analysed to evaluate the diversity of bacterial communities of LC-MFC and SL-MFC. The Dice index of similarity method was used as a band based nearest-neighbour correlation and UPGMA (average linking method) was used as part of the hierarchical clustering method (see Supplementary Information for further details).

3. Results

3.1. Comparative power production

The control algorithm, when applied to LC-MFC, regulates the load resistance at an appropriate level to maximise the power produced. Thus, the time evolution of the power in LC-MFC differs from the power in SL-MFC (Fig. 2). SL-MFC shows a rapid decrease of power over 100 h, tracking the voltage, as the load is constant (200 Ω). However, in the LC-MFC the power is affected by the control algorithm and remains relatively constant (∼35 μW) until approximately 250 h. The power increases dramatically to peak at 270 μW between 300 h and 400 h at which point substrate depletion begins to affect the power generation. At high rates of power generation, diurnal variations in temperature are observed to have a greater effect than when the power is lower. The regulation of power to maintain peak power, against temperature induced diurnal voltage variation is clearly evident in Fig. 2a between 100 h and 300 h. However, the power in the SL-MFC fluctuates in response to the changing ambient temperature as a consequence of voltage variations resulting from the fixed resistance (200 Ω). The effect of temperature on voltage generation is evident in the temperature dependence of the Nernst equation which governs the electrochemical reaction in MFCs, and variations in metabolic rates in the electroactive biofilm.

The peak power in the controlled system should be sustainable if substrate can be maintained and plausibly could allow the power to continue to increase to the point that a maximum power for a given system and biocatalyst may be achieved. In this batch experiment however, substrate depletion prohibits further increases in power and conversely the power decreases to ∼11 μW at time 530 h (COD, $17 \pm 2\ mg\ l^{-1}$). LC-MFC, which evidently tracks the internal impedance as well as the capacity of the biocatalyst to supply current, also shows a significantly higher average power generation when compared to SL-MFC. Fig. 2b and d show that the voltage and consequent power of SL-MFC decrease over the first 100 h of the batch experiment. When compared to LC-MFC in Fig. 2a and c, the voltage and power evolution over time differ markedly between the controlled and un-controlled MFCs, leading to a higher aggregated energy yield from LC-MFC.

3.2. Effect of temperature on controlled load

Fig. 3a shows the variations in load resistance effected by the control strategy in response to temperature (Fig. 3b) and other disturbances, as well as the capacity of the biocatalyst to generate current. The influence of the performance of the associated cathode has been simplified in the interest of clarity, by using of a strong liquid phase oxidant (ferricyanide).

It is clear from Fig. 3 that the metabolic and reaction rate variations caused by temperature fluctuations and consequently voltage (or power) generation can be recognized by the control algorithm. The control actions adjust power to a state close to its temporally varying local maximum. This can be seen from the strong correlation between the diurnal temperature fluctuations and the load resistance variations over the period of 100–300 h when substrate was sufficient for electrogenesis. Between 300 h and 400 h the power generation of LC-MFC shows an elevated level (average

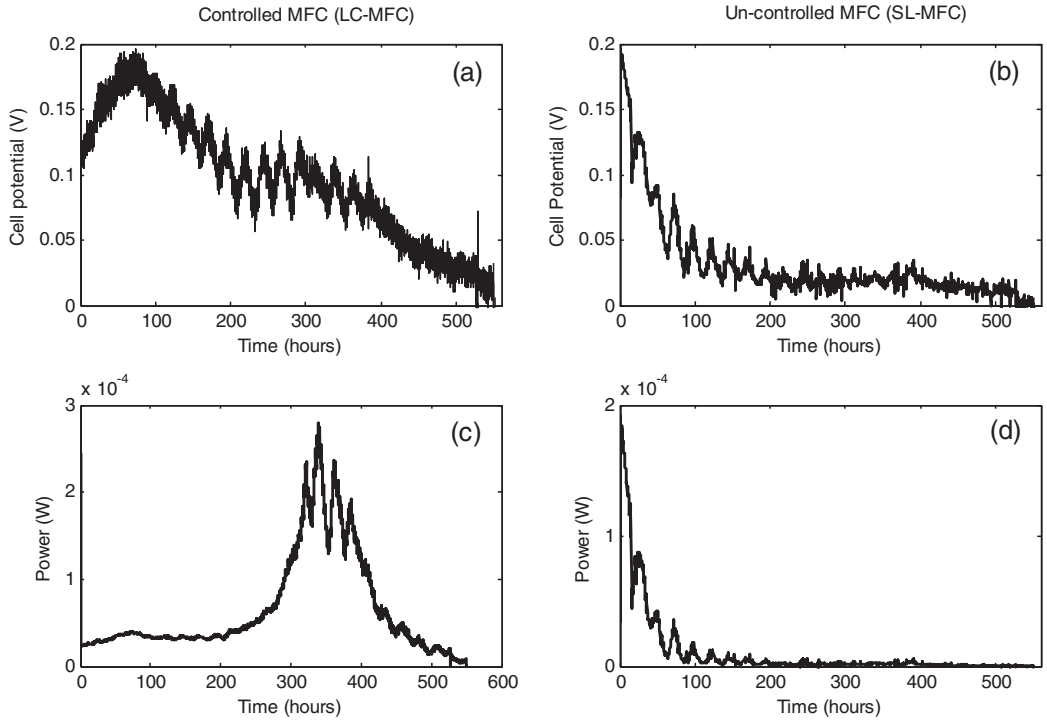

Fig. 2. Evolution of MFC potential and power generation in LC-MFC (a and c) load controlled and SL-MFC (b and d) un-controlled MFC (load is constant 200 Ω).

175 μW) with the load controlled below 90 Ω (average 44.2 Ω), as was shown in Fig. 2c. The power production in this period resulted from the relevant cell potential of LC-MFC (52–116 mV, average 85 mV). The average cell potentials between 0 h and 300 h and 400–550 h, were 129 mV and 55 mV respectively. This reducing trend in potential and the lowering of the load resistance indicates that the current is sourced from the biofilm at increased rates. This result implies that the power increase over SL-MFC performance is derived from improved electrogenic activity through control actions on LC-MFC, probably delivered through growth of electrogenic species and/or metabolic adaptation and flexibility of the anodic biofilm.

3.3. Coulombic efficiency (CE) of load controlled MFC

The instantaneous charge yield from the MFC, $C = i \cdot t$ (coulombs) was calculated at each sampling period and presented in Fig. 4. To better visualise the trend in this data, Fig. 4 also shows the same data, digitally filtered by a zero phase shifting bi-directional filter, designed using the Yule–Walker method as implemented using MatLAB™ and Signal Processing Toolbox©.

Integrating the instantaneous charge curve of Fig. 4a and b shows the cumulative charge that has been produced over the entire experiment in both the controlled (LC-MFC) and uncontrolled (SL-MFC) (Fig. 4c and d). It is possible to determine that

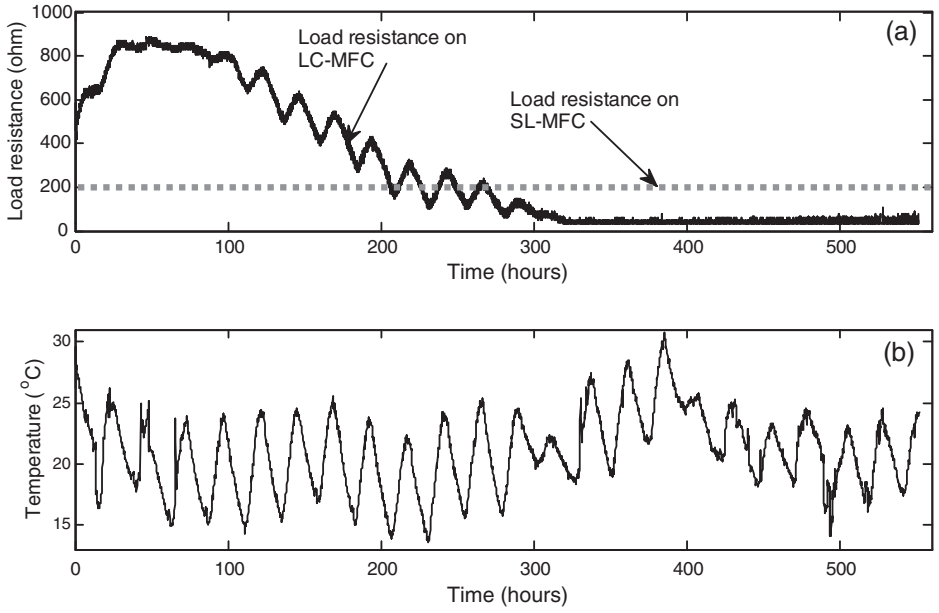

Fig. 3. Variation in (a) resistance commanded by the control algorithm (LC-MFC) and static load (SL-MFC) and (b) ambient temperature.

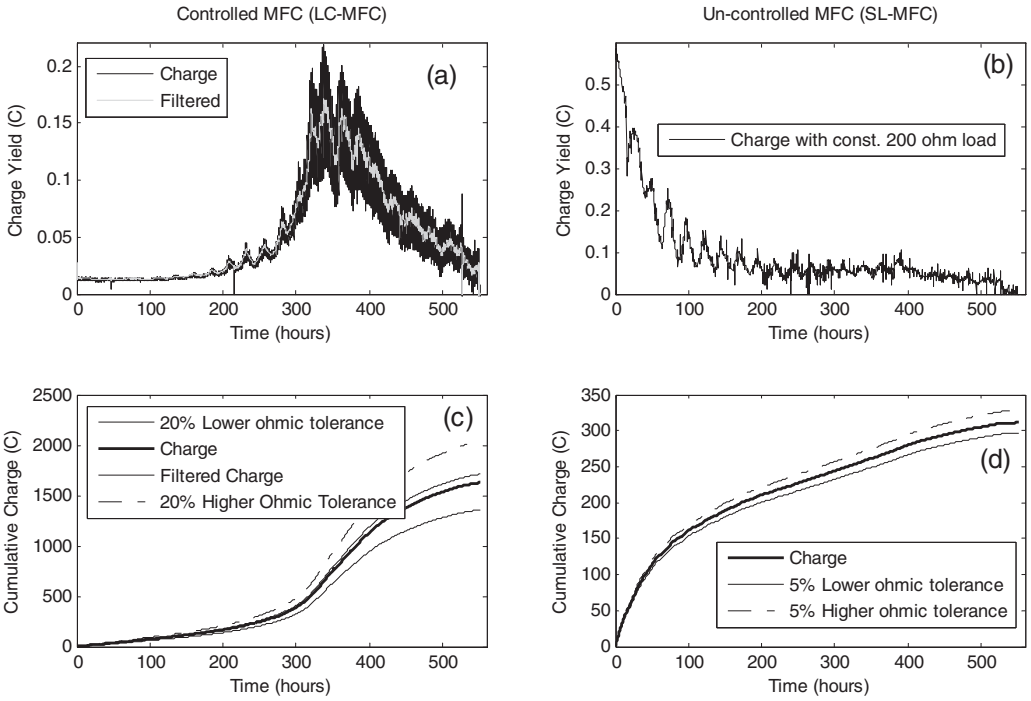

Fig. 4. Instantaneous and cumulative coulombic yields from controlled and un-controlled MFCs: (a) instantaneous generation of charge in controlled (LC-MFC); (b) instantaneous generation of charge in un-controlled (SL-MFC); (c) cumulative charge over 550 h experiment with controlled (LC-MFC), including potentiometer tolerances; (d) cumulative charge over 550 h experiment with un-controlled (SL547 MFC), including notional 5% tolerances on fixed resistance.

at approximately 250 h, the LC-MFC exceeds the cumulative energy production from the SL-MFC. It is also evident that the controlled system is able to increase the charge delivered compared to the un-controlled system by more than 1000 coulombs. Fig. 4c and d shows the worst case tolerance band of ±20% for the digital potentiometer (according to Intersil® X9Cxxx Data Sheet FN8222.1, 20th December, 2006) and an estimated ±5% aggregated tolerance for the fixed resistive load of the SL-MFC respectively.

The CE of LC-MFC in the controlled experiment 18.2% for the raw data (19.1% when filters as in Fig. 4a) and ranging from 15.1% to 22.8%, when considering the ±20% tolerance on load resistance on the X9C102 device. However, in the un-controlled MFC, the CE was 3.5% for the raw data and ranged from 3.3% to 3.7% (±5% tolerance on load resistance). This represents an increase in CE of between 11.5% at worst and 19.7% at best, which results from using load impedance (in fact, resistance) control (see Supplementary Information for further details on indicative repeatability).

3.4. Analysis of bacterial community composition by DGGE profile

Analysis of the DGGE profiles of bacteria and archaea reveals distinctively developed biofilms when comparing LC-MFC and SL-MFC (Fig. 5). Cluster Analysis was carried to analyse the similarity of band of biofilm on anode electrode and planktonic population of bacteria and archea. Fig. 5a indicates the similarity index of bacteria on biofilm between LC- and SL-MFC was relatively high (85.7%) as compared with that of suspension (64%). The similarity was more distinct in archaea (66.7% both in biofilm and suspension, Fig. 5b). This result indicates that the control action affects both bacterial and archeal community development, but archea are more affected by the load control which reflects the selective nature of the electrogenic growth in LC-MFC. This result also supports our previous finding of low coulombic efficiency of SL-MFC as compared with LC-MFC. Chae et al. [22] report that less methanogenic population (in gene copy number) was obtained in the lower resistance (50 Ω) than the higher resistance (600 Ω), implying that load affects methanogen development on anode electrode. Therefore, automatically optimizing control mechanism might successfully reduce non-electrogenic side reactions (e.g. methanogenesis and biomass production) and improve the performance of MFC. Further identification and analysis of the developed bacterial and archeal species with control mechanism might provide useful information of optimised electrogenesis in MFC.

The functional organisation of the bacterial biofilm communities was investigated through Pareto-Lorenz evenness plots (Fig. 6). The intercept from the 20% point (as indicated in Fig. 6) on the *x*-axis can be used as an evenness score, with the LC-MFC scoring 32% indicating a higher degree of evenness as compared with SL-MFC (48%). A high evenness value of 32% in the LC-MFC indicates a high functional spread of bacteria. This could suggest an increased functional flexibility to environmental change relating to the constant changes in external load resistance) initiated in LC-MFC compared to SL-MFC.

The total amount of biomass was monitored as an indicator of biological activity; specifically by quantifying the level of DNA present at the end of the experiment. The biomass present in the LC-MFC biofilm was observed to be less than half that in the SL-MFC biofilm (Table 2). The diversity of microbial (both archaeal and bacterial) species determined by Dice's index of similarity was observed to be higher in the LC-MFC than SL-MFC (bacterial community, 185.9 *cf.* 150.9; archaeal community, 73.5 *cf.* 43.4), further supporting the higher degree of flexible activity in the controlled reactor (as described above).

Table 2
Total biomass in LC-MFC and SL-MFC.

Reactor sample	Total biomass (DNA ng μl^{-1})
SL-MFC biofilm	314
LC-MFC biofilm	144
SL-MFC planktonic	3.5
LC-MFC planktonic	10.9

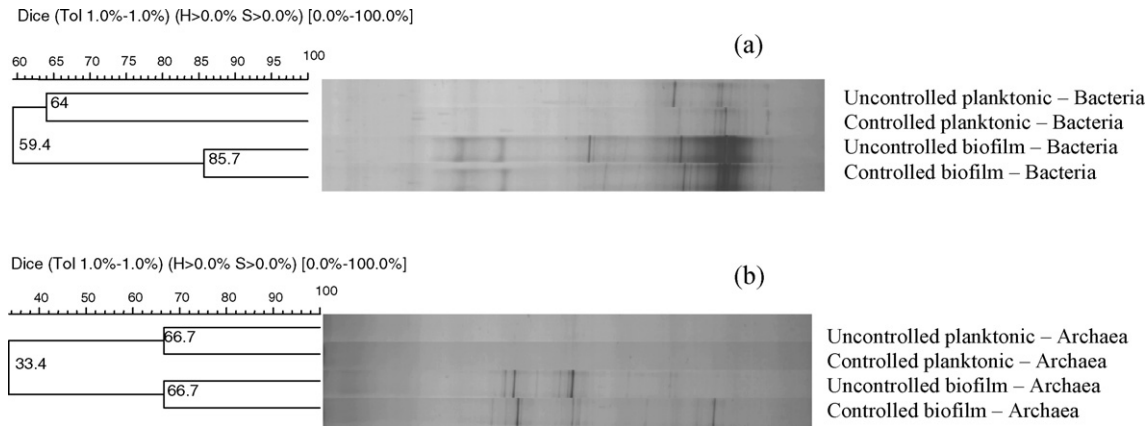

Fig. 5. DGGE bacterial and archaeal community profiles from controlled and un-controlled MFCs. Cluster analysis was carried out using the Dice coefficient of similarity measurement: (a) bacterial banding profile (LC-MFC and SL-MFC); (b) archaeal banding profile (LC-MFC and SL-MFC).

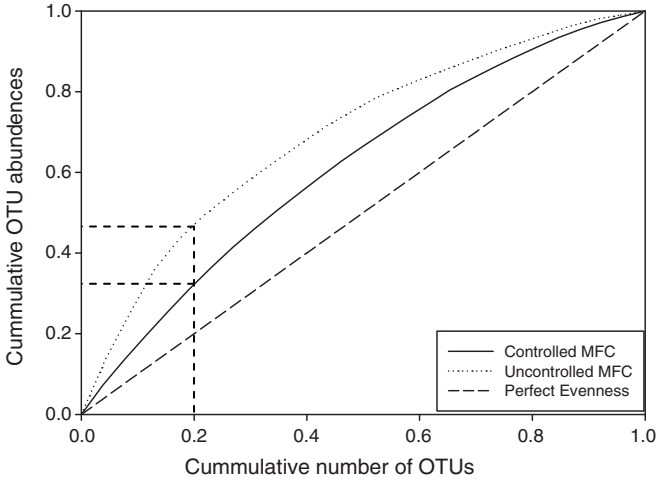

Fig. 6. Pareto-Lorenz evenness graph for LC-MFC and SL-MFC bacterial biofilm populations. DGGE bands profiles were ranked from high to low according to their cumulative intensities and cumulative number the of band results (scored using Dice's index of similarity).

4. Discussion

The control strategy used in this study is based on Boolean logic and is intended to be a parsimonious strategy. Improved power transfer is expected when internal and external impedances are matched, and the effectiveness of the biofilm to generate current shows improved performance when load control is applied. Simple, cost effective and low power consuming automatic control strategies may become highly desirable in implement MFC technology in wastewater treatment and bioenergy recovery. For these applications, hardware technologies such as microcontrollers, logic gates and programmable gate arrays could be utilised to control MFC reactors. Bespoke design may be necessary in order to optimise the harvesting of power, which effectively controls the current and potential from each MFC and simultaneously increases organic removal capacity. Variation of load impedance as a control mechanism must consider the end use of the power in any practical system, where the power from the MFC might initially be stored, or used directly to power an electrical load.

The resolution of the X9C102 was not high (10 Ω) in relation to the loading on the MFC (maximum reached, *circa* 700 Ω). However, this resolution was adequate for the useful investigation of the control strategy, in the context of 1 min sampling intervals with the load held constant in the interval between samples. The transient dynamic response of the MFC in relation to step changes in load has been estimated from observations during cyclic voltammetery and power curve characterisation, to have a time constant (assuming linear 1st order dynamics) of approximately 3–5 min (data not shown). The MFC process itself will therefore smooth (or filter) the step changes in load between samples, in order to maintain reasonably low amplitude voltage variations in response to each step change in load. The resolution of the X9C102 based load can be increased by operating two or more devices in parallel.

The substrate depletion and simultaneous cell potential decrease result in significantly different power generation between LC- and SL-MFCs. Fig. 2 clearly shows that SL-MFC could sustain the current demand for a period of approximately 4 days (∼100 h) with progressively impaired performance. This suggests that excessive and prolonged demand for power causes damage to the electrogenic activity and so reduces performance, i.e. without using automatic load adapting control. However, the cell potential of LC-MFC is sustained to a far greater extent even when the load resistance is diminished to draw the current, as a means of maximising the power from the MFC between 250 h and 350 h of operation (Figs. 2 and 3). The different performances of LC- and SL-MFCs in relation to substrate depletion implies that the automatic load control algorithm could successfully adapt to changes in environmental condition, and maintain near optimum performance to the point that there is insufficient substrate to sustain the process.

The cumulative charge produced by the SL-MFC tends to reach a lower plateau of 300 coulombs while the same substrate supply yields an approximately 5 times higher peak of cumulative coulombs in LC-MFC (Fig. 4). This increased coulombic output is directly proportional to increased CE of LC-MFC as compared to SL-MFC (18.2% and 3.5% respectively). Whilst the growth of biofilm is often associated with increased current densities [23], biomass accumulation can also be a significant electron sink along with other non-respiratory or side reactions such as methanogenesis [24], which then act to reduce CEs.

The relatively low CE in both MFCs can be attributed to the high initial concentration of acetate (5000 mg l^{-1}), with consequently longer batch operation time. There is therefore a high possibility of undesirable side reactions. The LC-MFC reactor in this experiment produced less than half the total biomass produced in the SL-MFC reactor (Table 2) but produced substantially more accumulated coulombic charge (Fig. 4).

The significantly higher CE of LC-MFC implies that automatic load control makes more electrons available from the substrate to electrogenic bacterial processes for electricity production in MFCs. It is reasonable to hypothesize that the control strategy imposed selective pressures favouring electrogenic species and

metabolic pathway in the biofilm, and impeding the unproductive non-electrogenic side reactions. The microbial composition analysis by DGGE band profile to support this hypothesis is described in the following paragraph.

Fig. 5 shows that the biofilm development is affected by the operational histories of LC- and SL-MFC. The DGGE profile analysis shows that control has resulted in clearly different ecologies in LC- and SL-MFCs. The continuous selective pressure is likely to be imposed on the ecology of LC-MFC, where the active biofilm is continually perturbed toward higher current yield, but loading is also adjusted to relieve unsustainable demand for current.

A similarity score of 85.7% between the LC-MFC and SL-MFC bacterial biofilm communities indicates that a common range of electrogenically active bacteria existed in both LC-MFC and SL-MFC, but differences in the operational conditions were also reflected in the development of distinct bands. Identification of the species was not conducted in this study, however it could provide more useful information for adaptive species on load controlled condition, and could possibly screen species with high electrogenic capability. Interestingly, the load control algorithm affects the archaea more significantly than bacterial population, as a lower similarity index (66.7%) was obtained (Fig. 5b). This result is consistent with results previously reported, indicating that the methanogenic population was affected by external load, and reduced methanogenesis was obtained at lower resistance and higher current [22].

The ability of the microbial community to adapt to maximum power production in LC-MFC would seem to be driven by microbial growth as this process took ~12 days (Fig. 2), as opposed to being solely an adjustment of bacterial metabolic pathways or different respiratory cytochromes. Therefore, the control as implemented in this study seems to promote the selection of more appropriate electrogenic ecologies.

5. Conclusions

The application of logic based control of external load resistance is able to increase the power and cumulative energy generated by an MFC as compared to an identical system which has a static resistive load. The LC-MFC generated maximum power of $12.4\,\mu W\,cm^{-2}$ and 1600 ± 400 C, while the SL-MFC generated maximum $8.4\,\mu W\,cm^{-2}$, 300 ± 10 C using the same concentration of substrate over the same time period and the comparative CE of the LC-MFC over the SL-MFC is shown to increase by between 11.46% at worst and 19.73% at best when considering tolerances ascribed to load resistances. The LC-MFC presented a CE of 18.15% for the raw data (19.07% when data was filtered) and ranging from 15.12% to 22.68%, depending on the X9C102 device ±20% tolerance on load resistance. In the SL-MFC, the CE was 3.47% for the raw data and ranged from 3.31% to 3.66% (±5% tolerance on load resistance).

The LC-MFC operated in a more stable manner than SL-MFC against environmental changes such as substrate depletion and temperature fluctuation. The increased power production, coulombic efficiency and operational stability of the LC-MFC over the SL-MFC were derived from the automatic control of a resistive load, which resulted in more efficient conversion of the substrate (fuel) to electricity, caused by the *quasi*-optimal loading presented to the LC-MFC.

The selective pressure on the biofilm of LC-MFC may be able to optimize the electrogenic biofilm and increase the performance of MFC system for power density and organic load removal. Further development of the control algorithm, giving consideration to operating condition and system configuration could facilitate MFC technology implementation into real-world applications such as wastewater treatment and bioenergy recovery.

Acknowledgements

This research was funded by the RCUK Energy Programme, SUPERGEN Biological Fuel Cell project (EP/D047943/1) supported by grant 68-3A75-3-150. The Energy Programme is an RCUK cross-council initiative led by EPSRC and contributed to by ESRC, NERC, BBSRC and STFC.

Appendix A. Supplementary data

Supplementary data associated with this article can be found, in the online version, at doi:10.1016/j.jpowsour.2010.09.071.

References

[1] J. Biffinger, M. Ribbens, B. Ringeisen, J. Pietron, S. Finkel, K. Nealson, Biotechnology and Bioengineering 102 (2009) 436–444.
[2] F. Zhao, F. Harnisch, U. Schroder, F. Scholz, P. Bogdanoff, I. Herrmann, Electrochemistry Communications 7 (2005) 1405–1410.
[3] D. Pant, G. Van Bogaert, L. Diels, K. Vanbroekhoven, Bioresource Technology 101 (2010) 1533–1543.
[4] P. Clauwaert, P. Aelterman, T.H. Pham, L. De Schamphelaire, M. Carballa, K. Rabaey, W. Verstraete, Applied Microbiology and Biotechnology 79 (2008) 901–913.
[5] A. Dekker, A. Ter Heijne, M. Saakes, H.V.M. Hamelers, C.J.N. Buisman, Environmental Science & Technology 43 (2009) 9038–9042.
[6] P. Aelterman, M. Versichele, M. Marzorati, N. Boon, W. Verstraete, Bioresource Technology 99 (2008) 8895–8902.
[7] D.A. Lowy, L.M. Tender, J.G. Zeikus, D.H. Park, D.R. Lovley, Biosensors & Bioelectronics 21 (2006) 2058–2063.
[8] F. Zhao, R.C.T. Slade, J.R. Varcoe, Chemical Society Reviews 38 (2009) 1926–1939.
[9] D.Y. Lyon, F. Buret, T.M. Vogel, J.M. Monier, Bioelectrochemistry 78 (2010) 2–7.
[10] L. Woodward, M. Perreir, B. Srinivasan, B. Tartakovsky, Biotechnology Progress 25 (2009).
[11] P. Aelterman, K. Rabaey, H.T. Pham, N. Boon, W. Verstraete, Environmental Science & Technology 40 (2006) 3388–3394.
[12] S.E. Oh, B.E. Logan, Journal of Power Sources 167 (2007) 11–17.
[13] R.P. Pinto, B. Srinivasan, M.F. Manuel, B. Tartakovsky, Bioresource Technology 101 (2010) 5256–5265.
[14] C. Picioreanu, I.M. Head, K.P. Katuri, M.C.M. van Loosdrecht, K. Scott, Water Research 41 (2007) 2921–2940.
[15] S. Woodcock, C.J. van der Gast, T. Bell, M. Lunn, T.P. Curtis, I.M. Head, W.T. Sloan, Fems Microbiology Ecology 62 (2007) 171–180.
[16] X. Wang, Y.J. Feng, N.Q. Ren, H.M. Wang, H. Lee, N. Li, Q.L. Zhao, Electrochimica Acta 54 (2009) 1109–1114.
[17] S. Srikanth, S.V. Mohan, P.N. Sarma, Bioresource Technology 101 (2010) 5337–5344.
[18] K.Y. Cheng, R. Cord-Ruwisch, G. Ho, Bioelectrochemistry 74 (2009) 227–231.
[19] J.R. Kim, G.C. Premier, F.R. Hawkes, J. Rodriguez, R.M. Dinsdale, A.J. Guwy, Bioresource Technology 101 (2010) 1190–1198.
[20] J.R. Kim, J. Dec, M.A. Bruns, B.E. Logan, Applied and Environmental Microbiology 74 (2008) 2540–2543.
[21] K. Roest, H. Heilig, H. Smidt, W. Vos, A. Stams, A. Akkermans, System Applied Microbiology 28 (2005) 175–185.
[22] K.J. Chae, M.J. Choi, K.Y. Kim, F.F. Ajayi, W. Park, C.W. Kim, I.S. Kim, Bioresource Technology 101 (2010) 5350–5357.
[23] C.I. Torres, R. Krajmalnik-Brown, P. Parameswaran, A.K. Marcus, G. Wanger, Y.A. Gorby, B.E. Rittmann, Environmental Science & Technology 43 (2009) 9519–9524.
[24] B. Virdis, K. Rabaey, Z.G. Yuan, R.A. Rozendal, J. Keller, Environmental Science & Technology 43 (2009) 5144–5149.